

# Edge and scrape-off-layer instability and transport physics for NSTX

J. R. Myra, D. A. D'Ippolito  
*Lodestar Research Corporation*

X. Q. Xu  
*Lawrence Livermore National Laboratory*

June 2001  
revised August 2001

---

DOE/ER/54593-01

LRC-01-82

---

**LODESTAR RESEARCH CORPORATION**  
*2400 Central Avenue*  
*Boulder, Colorado 80301*

# Edge and scrape-off-layer instability and transport physics for NSTX

J. R. Myra, D. A. D'Ippolito

*Lodestar Research Corp., 2400 Central Ave. P-5, Boulder, Colorado 80301*

X. Q. Xu

*Lawrence Livermore National Laboratory, Livermore, CA 94550*

## Abstract

Gas puff imaging (GPI) experiments on the National Spherical Torus Experiment (NSTX) have shown that filamentary turbulent “blobs” exist in the vicinity of the separatrix. While it is expected that comprehensive modeling of the GPI data will require the use of three dimensional turbulence codes such as BOUT, it is shown here that a linear analysis of the instabilities in the separatrix region using the BAL code is capable of recovering the qualitative features of the observations to date, such as the scale size and characteristic frequency width of the turbulent spectrum. Predictions for the scaling of these quantities with safety factor  $q$ , magnetic field  $B$  and ion species (fueling gas) are made. In addition it is shown that the SOL is expected to be more quiescent in inner wall limited discharges relative to the double null configuration. Finally, it is speculated that edge turbulence may be suppressed in a high performance regime with high edge beta and steep pedestals. The relationship of the BAL code predictions to a recently developed convective transport (“blob”) theory is discussed.

## I. Introduction

It is commonly believed that the separatrix region of toroidal confinement devices can control both the global transport and confinement (e.g. the L-H transition), and the properties of the scrape-off-layer (SOL) which are critical to successful power handling, impurity control and plasma exhaust. These considerations, developed largely from experience with tokamaks, are no less critical for the successful operation of spherical tori (ST) such as the National Spherical Torus Experiment (NSTX).<sup>1,2</sup> In fact, because of the larger surface to volume ratio in an ST, edge physics effects are arguably even more important than in high aspect ratio tokamaks. Transport generated by turbulent processes is expected to set the SOL width and is therefore important for heat exhaust. Handling of the heat exhaust is expected to be a significant issue when NSTX operation at full power commences. Furthermore, characterization of plasma conditions in the SOL is necessary for optimizing high harmonic fast wave (HHFW) coupling and surface interactions on rf launching structures.

Recent experiments using gas puff imaging (GPI)<sup>3</sup> are very promising as a diagnostic of fluctuations in the separatrix region of NSTX. In the GPI experiments on NSTX,<sup>4,5</sup> a small amount of neutral gas is puffed through a 30 cm manifold and the resulting visible light emission is viewed by a fast camera (gate time  $\sim 10 \mu\text{s}$ , with 1 ms between frames) either along a magnetic field line (radial – poloidal plane) or across the field lines. The observations show strong filamentation of the visible light emission which is aligned along the magnetic field lines. In the radial-poloidal plane, these filaments appear as emission “blobs” or “wavy eddies” which are interpreted as primarily density fluctuations in the separatrix region. [The light emission is proportional to  $n_e n_0 f(n_e, T_e)$  where  $f$  and  $n_0$  are typically slowly varying in space and time.] The typical scale size of these fluctuations is 5 cm radially and 5 – 10 cm poloidally. High time

resolution (500 kHz) time series analysis data is also taken for a small spatial sample and indicates autocorrelation times on the order of 30  $\mu$ s, and broadband frequency spectra with a characteristic width on the order of 100 kHz.

On the theoretical front, a number of tools and conceptual developments are becoming available to model and interpret the GPI data. There is a growing optimism that ultimately these tools, described in the following, will be instrumental in putting together both conceptual and predictive models of turbulence and transport in the edge and SOL regions.

A very sophisticated modeling tool for turbulence of the edge and SOL region is the BOUT code<sup>6</sup> developed at LLNL. BOUT is a two-fluid, three-dimensional turbulence code which solves the Braginskii equations in X-point geometry, including both open and closed surfaces that span the separatrix region. Initial comparison of BOUT results with the NSTX experiment have yielded qualitative, and in some cases, quantitative agreement; *viz.* the frequency spectra, filamentary structure and eddy scale sizes are similar.<sup>7</sup> A definitive quantitative comparison awaits the availability of better characterization of the NSTX edge plasma, to use as input to the BOUT code.

The BAL linear stability code<sup>8</sup> developed at Lodestar, as well as analytical theory, have been important in understanding the unstable modes in X-point geometry and the corresponding turbulence seen in the BOUT code. BAL is a linear eigenvalue code, implemented within the eikonal ballooning formalism, that can treat both the closed and open flux surface regions in X-point geometry, including the physics of pressure driven modes, drift and resistive physics and divertor plate sheaths. The BAL code employs the same magnetic geometry model and input files that are used by BOUT.

While it is expected that comprehensive modeling of the GPI data will require the use of three dimensional turbulence codes such as BOUT, it is shown here that a linear analysis of the instabilities in the separatrix region using the BAL code is also capable of

recovering the qualitative features of the observations to date, such as the scale size and characteristic frequency width of the turbulent spectrum. It is of considerable interest to determine whether the observed GPI blob scales are essentially controlled by the parameters of linear theory, or whether there are fundamentally nonlinear scales. Motivated by this, we present here a BAL analysis of the predicted scaling of the features of the edge turbulence with safety factor  $q$ , magnetic field  $B$  and ion species (fueling gas). Corresponding scaling experiments are planned for NSTX in the near future.<sup>9</sup>

In addition, comparisons of NSTX magnetic configurations have been made. It is shown that the SOL is expected to be more quiescent in inner wall limited discharges relative to the double null configuration. Finally, it is speculated that edge turbulence may be suppressed in a high performance regime with high edge beta and steep pedestals.

These types of analyses, while possible in principle with BOUT, are comparatively very time consuming because of the massive CPU requirements for 3D edge turbulence simulations. The BAL code, on the other hand, is relatively well suited to scaling studies and to accessing the underlying physical nature of unstable edge modes. As in previous studies,<sup>8</sup> BAL and BOUT complement each other well for the NSTX work.

The question of how edge density fluctuations relate to transport in the SOL has received considerable attention. A review of the relevant literature is not possible here. However, recent developments in the theory of convective transport in the SOL may be of particular interest in interpreting the GPI data. It was initially proposed by Krasheninnikov<sup>10</sup> that non-diffusive transport in the SOL, as observed at least in some situations on many devices, could be mediated by density “blobs”. These blobs, or local enhanced regions of density in the radial-poloidal plane (with extended structure along  $B$ ), could detach from the main plasma and propagate across the SOL to the outer walls of the device due the curvature-induced charge polarization and resulting  $E \times B$  radial drift.

This convective transport model is in contrast to the usual picture where the SOL width is set by the balancing of radial diffusion by parallel flow into the divertor region. Further analysis<sup>11</sup> has begun to explore the properties of blobs in a Braginskii model including the role of vorticity and ionization. It has been shown that the SOL scale length depends on the blob distribution and detailed analysis gives rise to critical exponents for power law distributions of the blob size.<sup>11</sup>

The plan of our paper is as follows. In Sec II we present the results of the BAL code analysis for parameters typical of the NSTX boundary plasma. In Sec. III a discussion of the significance of these results and possibilities for future analysis of the NSTX GPI data is given. Finally, our conclusions are summarized in Sec. IV.

## **II. BAL code analysis of NSTX edge plasmas**

### *A. Basic physics, typical frequencies and scale lengths*

The reduced Braginskii model employed for the studies reported on here is given in Ref. 8. The model supports ideal (MHD), resistive (RMHD) magnetohydrodynamic instabilities, drift instabilities and sheath-driven instabilities (in the SOL). We employ an EFIT representation of the magnetic geometry, using an NSTX double null configuration as our base case.

A complete characterization of the NSTX edge and SOL plasmas by direct experimental measurements has not yet been possible. For these preliminary studies, we assume a hyperbolic tangent shape for the density and temperature profiles, specifying values for the pedestal width, and the density and temperature at the top and bottom of the pedestal. Unless otherwise noted, we run BAL on a flux surface just inside the separatrix (either 0.3 or 1 cm as measured at the outboard midplane) where the following best-guess

plasma parameters have been employed:  $n_e = 3.5 \times 10^{12} \text{ cm}^{-3}$ ,  $T_e = T_i = 40 \text{ eV}$ , and  $L_n = L_{Te} = L_{Ti} = 2.5 \text{ cm}$ .

A typical unstable spectrum is shown in Fig. 1 where the growth rate and real frequency of the fastest growing mode are plotted against toroidal mode number  $n$ . It is seen that the edge instabilities are in the frequency range  $|\omega| < 700 \text{ krad/s}$  corresponding to  $|f| < 100 \text{ kHz}$ . This is precisely the range of the turbulent spectrum seen in the time series analysis GPI data. Furthermore, the BAL code peak growth occurs at  $n = 172$  with  $f = 46 \text{ kHz}$  and yields cross-field scale lengths of order  $L_{\theta 0} = 2\pi/k_{\theta 0} = 4.4 \text{ cm}$  where  $k_{\theta}$  varies along the field line in X-point geometry, and  $k_{\theta 0}$  is referenced to the outboard midplane. This scale length is also typical of the GPI data.

While a linear code cannot directly predict a saturated turbulent spectrum, we envision that the spectrum of Fig. 1 is filled by nonlinear mode coupling and turbulent broadening processes driven by the energy of the fastest growing mode. Thus we expect that the nonlinear spectrum will qualitatively display the scalings and characteristics dictated by the underlying physics of the modes, here dominated by drift and curvature physics. The predictions of this *ansatz* are given in the subsections that follow, and their validity will be testable by future GPI data.

### ***B. Scaling with safety factor $q$***

The unstable modes in the NSTX edge plasma are driven by a combination of resistive (RMHD) and drift-wave physics. Some intuition regarding the scaling of the unstable spectrum with respect to variations in  $q$  and  $B$  may be obtained by considering the pure resistive limit, first neglecting drift ( $\omega_{*i}$ ,  $\omega_{*e}$ , and  $k_{\perp}\rho_s$ ) effects. For a circular flux surface model, the modes in this RMHD limit are the Carreras-Diamond (CD) modes<sup>12</sup> which scale like  $\gamma \sim q^{4/3} n^{2/3}$ . In X-point geometry, the CD modes are modified because for the parameters given (indeed for almost all interesting edge

parameters) the so called “two-scale approximation” breaks down,<sup>13</sup> viz. the eigenfunctions are strongly modified as they pass near the X-point and do not remain nearly interchange-like as in the original CD theory. This behavior, seen in the BOUT and BAL codes, is that of a mode whose physics is strongly influenced by X-point physics: the resistive X-point class of modes.<sup>6,8</sup> Furthermore, RMHD is not a good model for NSTX because the relatively small outboard magnetic field makes for large Larmor radii and correspondingly increases the importance of drift physics.

Nevertheless, certain features extracted from the CD theory turn out to apply in the present situation. At sufficiently low mode numbers, where drift effects are relatively unimportant the growth rate  $\gamma$  increases with  $q$ . Because drift physics tends to favor instabilities at fixed  $k_\theta \rho_s \propto nq$ , higher  $q$  shifts the peak growth rate to lower  $n$ . These features are evident in Fig. 2 which shows the unstable spectrum for the base case, and for a case with  $q$  increased by a factor of two. The results show that the most unstable  $n$  scales more strongly than  $1/q$  implying that the fastest growing  $k_\theta \propto nq$  is somewhat reduced for the high  $q$  case. The magnetic geometry for the case with increased  $q$  was obtained employing the base case flux surface shape and toroidal magnetic field, but reducing the plasma current by a factor of two before constructing the field lines and curvature components required for the BAL analysis.

Thus linear theory predicts that the poloidal scale size of the turbulence will get somewhat larger at high  $q$ . From the real frequency spectrum (not shown) it is also deduced that the characteristic frequencies will be lower at high  $q$ .

### ***C. Scaling with magnetic field $B$***

The scaling of the unstable spectrum with magnetic field  $B$  is shown in Fig. 3. The safety factor  $q$ , as well as the flux surface shape were held constant in the comparison. It can be shown that the CD modes have  $\gamma \sim 1/B^{2/3}$  and the figure shows



that this scaling persists, at least qualitatively, in X-point geometry for sufficiently low  $n$ . As in the  $q$  scaling study, drift physics becomes dominant at larger  $n$ , and controls the physics of the peak of the  $\gamma(n)$  curve. The case with reduced  $B$  is seen to have a spectrum that shifts to lower  $n$ , consistent with  $k_\theta \rho_s \propto n/B$ . It will also be noted that the value of the growth rate at the peak is reduced, probably due to the competition of stabilizing FLR (at high  $n$ ) and resistivity (necessary for mode growth, but small at low  $n$ ). Additionally there is increased finite  $\beta$  drift wave stabilization in the reduced  $B$  case. Note that the reduction in  $\gamma$  accompanying the shift to lower  $n$  is in contrast with the  $q$  scaling where there is compensation in the increased connection lengths at high  $q$  – physics which decreases the stabilizing line bending energy and therefore acts to enhance the growth rate.

Thus linear theory predicts that the scale size of the turbulence will get larger at low  $B$ . From the real frequency spectrum (not shown) it is also deduced that the characteristic frequencies will be similar (perhaps very slightly lower) at low  $B$ . From the value of the peak  $\gamma$ , we speculate that the fluctuation levels may be more reduced in scaling to low  $B$  than in scaling to high  $q$ , however this prediction of linear theory is subject to more uncertainty because the nonlinear physics of saturation may be different in the two cases.

While the scalings with  $B$  and  $q$  are of interest from a theoretical perspective, it is easier experimentally to vary the toroidal field  $B_\zeta$  holding the plasma current  $I_p$  and hence the poloidal field  $B_\theta$  constant. We have also performed this scaling comparison numerically, The results are shown in Fig. 4. Since  $k_\theta \propto nB_\zeta$ , and the peak  $n$  is essentially constant, the case with reduced  $B_\zeta$  yields instabilities at smaller  $k_\theta$ . Thus, smaller  $B_\zeta$  implies smaller growth rates and larger poloidal scale lengths (provided the plasma parameters are indeed constant in the two cases, which presents a separate

experimental difficulty). Not shown, is the code prediction that the frequency will increase in the lower  $B_\zeta$  case.

#### ***D. Scaling with ion species: $Z$ and $\mu$***

As a final scaling study, we consider the effect of the ion charge  $Z$  and atomic mass number  $\mu$ . Results for three plasma compositions are shown in Fig. 5. In these studies, the electron density  $n_e$  is held fixed as  $Z$  varies. It is seen that the peak growth rates and corresponding mode numbers increase in the sequence D,  $^4\text{He}$ ,  $^3\text{He}$  with  $^4\text{He}$  and  $^3\text{He}$  being similar. An examination of the theory shows that the main dependences on  $Z$  and  $\mu$  enter through the Alfvén velocity  $v_a \sim (Z/\mu)^{1/2}$ ,  $\rho_s \sim \mu^{1/2}/Z$ , and  $v_{ei} \sim Z$ . Again, the  $n$  corresponding to the peak  $\gamma$  is consistent with constant  $k_\theta \rho_s \propto n\mu^{1/2}/Z$ . The value of the peak  $\gamma$  qualitatively has the scaling of the collisional drift-Alfvén mode,  $\gamma \sim Z^{7/4}/\mu^{3/4}$ .

Thus linear theory predicts that the scale size of the turbulence will get smaller in He relative to D. From the real frequency spectrum (not shown) it is also deduced that the characteristic frequencies will be slightly higher in He plasmas.

#### ***E. Speculation on high performance discharges***

While there are a number of challenges to be faced in the future, the initial success of NSTX in establishing and heating well-confined plasmas suggests an optimism that high performance regimes may be attainable in NSTX and in STs in general. Motivated by this, we considered a case employing high edge  $\beta$  and a very steep high pressure edge pedestal. In this situation, large  $\rho_i/L_n$  stabilizes the resistive curvature driven modes by finite Larmor radius (FLR) physics, while high edge  $\beta$  stabilizes the drift-Alfvén modes.

The former condition has been discussed by Rogers et al. in the circular flux surface case<sup>14</sup> and leads to the condition  $\alpha_d > 1$  where

$$\alpha_d = \frac{c_s \rho_s v_a}{q R L_n \delta_e v_{ei} \gamma_{\text{mhd}}^{3/2}} = 3.8 \times 10^6 \frac{L_p^{3/2} T}{L_n n_e^{1/2} q R^{1/4}} \quad (1)$$

and  $\gamma_{\text{mhd}}^2 = 2c_s^2 / RL_p$ . Here, in X-point geometry, the proper definition of  $\alpha_d$  is not obvious since the effect of the X-point is to make resistive effects much more important than in the circular case.<sup>8</sup> Nevertheless, the essential physics is clear: FLR stabilizes the high- $n$  modes that would otherwise be subject to RMHD instability. The latter condition, finite  $\beta$  stabilization of the drift-Alfvén modes, requires that

$$\beta > \frac{m_e}{m_i} \quad (2)$$

or equivalently that

$$\rho_s > \delta_e \quad (3)$$

where  $\delta_e = c/\omega_{pe}$  is the electron skin depth.<sup>15</sup>

For this high-performance plasma study, we employed the illustrative base case parameters  $n_e = 3.6 \times 10^{12} \text{ cm}^{-3}$ ,  $T_e = T_i = 120 \text{ eV}$ , and  $L_n = L_{Te} = L_{Ti} = 0.8 \text{ cm}$ . Because of the steep edge gradient, the local eikonal theory implemented in the BAL code is questionable in this regime; however, as will be apparent, the results are sufficiently interesting to justify their inclusion here.

In a sequence of runs where the pressure was systematically increased from the high-performance base case parameters just given, we found that there was a transition to a stable edge. Results are shown in Fig. 6. The base case has  $\rho_s/\delta_e = 1.9$ , and the subsequent cases correspond to an increase in the pressure by an additional factor of 3 ( $\rho_s/\delta_e = 3.2$ ) and 6 ( $\rho_s/\delta_e = 4.6$ ).

The prediction of linear theory from these runs is that edge characteristics (i.e. turbulent fluctuation levels) may improve as high  $\beta$  steep edge pedestal regimes are accessed. If so, this would further promote the self-consistent maintenance of the steep

pedestal, transport barrier region. We note that the regime of high edge  $\beta$  and large  $\rho_i$  on the outboard side of the torus is well suited to the ST concept.

### ***F. Comparison of double null and inner wall limited configurations***

To illustrate the role of the edge magnetic geometry on the instabilities, we compare the stability of the SOL for the double null (DN) base case with an inner wall limited case. For sample NSTX SOL parameters ( $n_e = 1.1 \times 10^{12} \text{ cm}^{-3}$ ,  $T_e = T_i = 38 \text{ eV}$ , and  $L_n = L_{Te} = L_{Ti} = 3 \text{ cm}$ ), the modes tend to have an interchange structure that allows them to contact the divertor plates or inner wall on which the field lines terminate. At higher values of plasma resistivity (e.g. when the density is increased) the X-point can effectively isolate the modes from the sheath boundary conditions that apply on the open field lines.<sup>8,13</sup> In the present runs, this isolation was not complete, and the boundary conditions were found to play an important role in determining the SOL stability.

The results illustrated in Fig. 7 show that that inner wall limited (main outboard) SOL is more stable than the main outboard SOL in the DN configuration. The explanation is simply that the modes see good curvature on the inside of the torus in the inner wall limited case, and this leads to smaller growth rates.

Thus linear theory predicts a more quiescent SOL in the inner wall limited configuration, relative to the DN case.

## **III. Discussion and significance for GPI data analysis**

The BAL code analysis and scaling arguments presented in the preceding section provide an important experimental test of edge turbulence models and, when combined with recently developed blob theory,<sup>10,11</sup> could lead to the development of significant insights on the physics of the SOL width and SOL transport. A working hypothesis, subject to future experimental verification on NSTX, is that SOL blobs originate from

unstable modes in the pedestal/separatrix region which produce saturated eddies and then break away into the SOL as blobs. The tendency of blobs to break away arises as a natural consequence of the blob's outward radial velocity discussed subsequently.

In blob theory,<sup>10,11</sup> the size of the blobs is a crucial parameter. The density blobs experience charge polarization due to the opposite curvature drift of electrons and ions. This produces a local poloidal electric field in the blob that causes the blob to move radially outward due to the  $E \times B$  drift. Thus, blob theory gives the result that the radial blob speed across the SOL is determined by the blob size, which in turn, in our hypothesis, is determined by the turbulent eddy size scaling discussed in Sec. II. These predictions of eddy size scalings can be tested experimentally by measuring the size and/or speed of blobs from GPI or probe data.

Furthermore, in blob theory, the blob speed and decay rate determine the SOL scale length. The decay rate is determined by the parallel loss of particles to the sheaths less compensation from the particle source implied by ionization of neutrals. An independent measure of the SOL scale length would allow the blob theory of non-diffusive SOL transport to be tested. Success in correlating the eddy size with the SOL scale length would be a significant step in understanding and controlling the SOL to optimize performance and exhaust handling

## **IV. Conclusions**

The BAL code studies described in this report give predictions for the scaling of the fluctuation frequency spectrum and scale size of the edge turbulence (eddies or blobs) with the variation of  $q$ ,  $B$ , and ion species. In summary we find that the poloidal scale size of the eddies (approx 4 cm for the base case) will increase at high  $q$  and low  $B$ . The characteristic frequency of the turbulent spectrum (100 kHz for the base case) will be reduced at high  $q$  but will stay similar (perhaps be very slightly reduced) at low  $B$  when  $q$

is fixed. If  $B_\zeta$  is varied at fixed  $I_p$ , the frequency will increase at lower  $B_\zeta$ . There is some evidence that the fluctuation levels may be reduced in the low B case relative to the high q case. It is predicted that fluctuations will be similar in  $^4\text{He}$  and  $^3\text{He}$ , and that the scale size of the turbulence will be smaller in He plasmas relative to D. Also, the frequencies are expected to be slightly higher in He than in D. These scalings may be qualitatively understood from a careful consideration of both RMHD physics (specifically the Carreras-Diamond modes) and, more importantly, the scaling of  $k_\theta \rho_s$  which embodies the drift wave physics that is so important in the NSTX edge plasma.

We have shown that the SOL is expected to be more quiescent in the inner wall limited configuration, relative to the DN case. We have also made some speculations on the favorable stabilization effects that may arise as high  $\beta$  steep edge pedestal regimes are accessed.

The calculations agree qualitatively with available GPI data taken to date on the base case eddy scale size and characteristic frequency of the turbulent spectrum. Experiments planned for the near future will determine whether the predicted scalings are in fact observed, and by implication, whether the existing models and understanding of the edge instabilities and turbulence are on a solid footing. Tests of the scalings presented here will help to answer the important question of whether the blob space and time scales are essentially controlled by the parameters of linear theory, or whether there are fundamentally nonlinear scales. This will shed insight on the physics that creates the blobs, and how they, and the resulting transport, can be controlled in an operational sense. Some ideas for extending the analysis and interpretation of GPI data to understand the effect of blob sizes (and corresponding radial velocities) on the SOL width have been presented.

## **Acknowledgments**

The authors wish to thank R. Maqueda, S. Zweben, and S. Kaye for providing NSTX geometry and boundary plasma data, and for enlightening discussions of the NSTX experiment and the GPI data. This work was supported by U.S. Department of Energy (DOE) under grants DE-FG03-00ER54593 and DE-FG03-97ER54392 and contract W-7405-ENG-48; however, such support does not constitute an endorsement by the DOE of the views expressed herein.

## References

- 1 S. Kaye et al., *Fusion Technology* **36**, 16 (1999); and S. Kaye et al. in *Proceedings of the Current Trends in International Fusion Research*, (2001).
- 2 M. Peng, *Plasma Phys* **7**, 1681 (2000).
- 3 S.J. Zweben and S.S. Medley, *Phys Fluids* **B1**, 2058 (1989).
- 4 R.J. Maqueda, G.A. Wurden, S. Zweben et al, *Rev. Sci. Instruments* **72**, 931 (2001).
- 5 S. Zweben, R. Maqueda, K. Hill, D. Johnson, S. Kaye et al., presented at the *EPS 27th Conference on Controlled Fusion and Plasma Physics*, Budapest, Hungary (2000), paper P2.118.
- 6 X.Q. Xu et al., *Phys. Plasmas* **7**, 2290 (2000) and refs. therein.
- 7 X.Q. Xu et al., presented at the *2001 International Sherwood Fusion Theory Conference*, April 2 – 4, 2001, Santa Fe, New Mexico, paper 2B02.
- 8 J.R. Myra, D.A. D'Ippolito, X.Q. Xu and R.H. Cohen, *Phys. Plasmas* **7**, 4622 (2000) and refs. therein.
- 9 R.J. Maqueda, S. Zweben, and S. Kaye, private communication (May 2001).
- 10 S.I. Krasheninnikov, *Phys. Lett. A* **283**, 368 (2001).
- 11 D.A. D'Ippolito, J.R. Myra and S. Krasheninnikov, presented at the *2001 International Sherwood Fusion Theory Conference*, April 2 – 4, 2001, Santa Fe, New Mexico, paper 1C14.
- 12 B.A. Carreras, P.H. Diamond et al., *Phys. Rev. Lett.* **50**, 503 (1983); T.C. Hender, K. Grassie and H.-P. Zehrfeld, *Nucl. Fusion* **29**, 1459 (1989).
- 13 J.R. Myra, D.A. D'Ippolito, X.Q. Xu and R.H. Cohen, *Contrib. Plasma Physics* **40**, 352 (2000).
- 14 B.N. Rogers and J.F. Drake, *Phys. Rev. Lett.* **81**, 4396 (1998).



- <sup>15</sup> A.B. Mikhailovskii, Nucl. Fusion **12**, 55 (1972); R.R. Dominguez, Nucl. Fusion **19**, 105 (1979).

## Figure captions

1. Typical growth rate  $\gamma$  ( $10^3/s$ ) and frequency  $\omega$  ( $10^3/s$ ) vs.  $n$  for the NSTX double null (DN) base case on a flux surface at  $x = -1$  cm. Peak growth occurs at  $n = 172$  with  $\omega = -292$  krad/s ( $f = 46$  kHz), implying  $k_{\theta 0} \rho_s = 0.52$  ( $k_{\theta 0} = 1.4$  cm $^{-1}$  and  $L_{\theta 0} = 2\pi/k_{\theta 0} = 4.4$  cm).
2. Scaling of the unstable spectrum with  $q$ . Shown is the growth rate  $\gamma$  ( $10^3/s$ ) vs.  $n$  for the base case and for a case with plasma current  $I_p$  reduced by a factor of 2 (i.e.  $q$  increased by 2). The flux surface is at  $x = -0.3$  cm for this and subsequent scaling runs.
3. Scaling of the unstable spectrum with  $B$ . Shown is the growth rate  $\gamma$  ( $10^3/s$ ) vs.  $n$  for the base case and for a case with toroidal magnetic field  $B$  reduced by a factor of 2. Here  $q$  is held constant.
4. Scaling of the unstable spectrum with  $B_\zeta$  at fixed  $I_p$ . Shown is the growth rate  $\gamma$  ( $10^3/s$ ) vs.  $n$  for the base case and for a case with toroidal magnetic field  $B_\zeta$  reduced by a factor of 2.
5. Scaling of the unstable spectrum with  $Z$  and  $\mu$ . Shown is the growth rate  $\gamma$  ( $10^3/s$ ) vs.  $n$  for various ion species. The base case (D) and cases for pure  $^4\text{He}$  and  $^3\text{He}$  plasmas are shown. Here  $n_e$  is held constant.
6. Growth rate  $\gamma$  ( $10^3/s$ ) vs.  $n$  for a sequence of runs with increasing pressure (edge  $\beta$ ), starting from the high-performance (high  $\beta$ , steep pedestal) parameters given in Sec. IIE.
7. Dependence of the unstable spectrum on magnetic configuration. Shown is the growth rate  $\gamma$  ( $10^3/s$ ) vs.  $n$  for the DN base case, and for an inner wall limited case on a typical flux surface ( $x = 1$  cm) in the SOL.

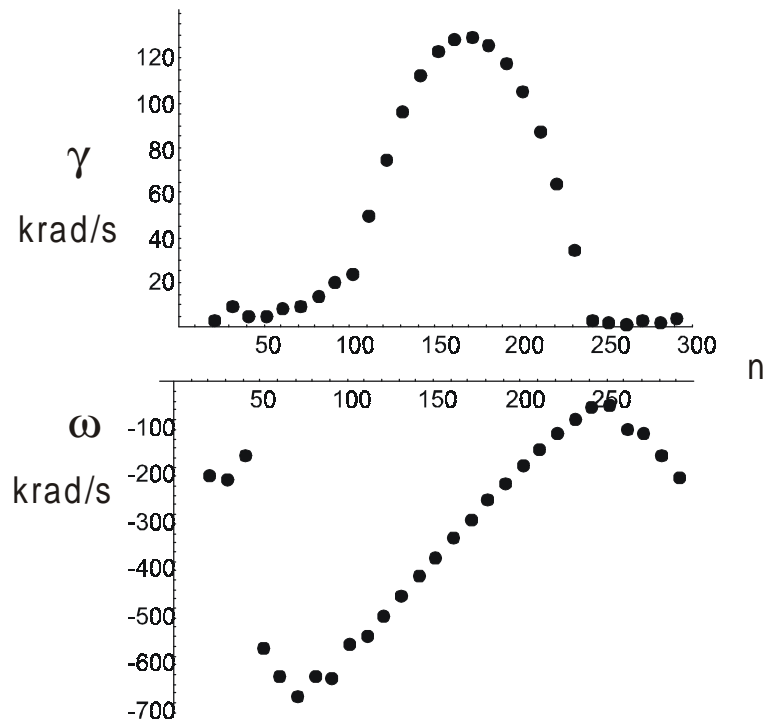


Fig. 1

Typical growth rate  $\gamma$  ( $10^3/s$ ) and frequency  $\omega$  ( $10^3/s$ ) vs.  $n$  for the NSTX double null (DN) base case on a flux surface at  $x = -1$  cm. Peak growth occurs at  $n = 172$  with  $\omega = -292$  krad/s ( $f = 46$  kHz), implying  $k_{\theta 0} \rho_s = 0.52$  ( $k_{\theta 0} = 1.4 \text{ cm}^{-1}$  and  $L_{\theta 0} = 2\pi/k_{\theta 0} = 4.4$  cm).

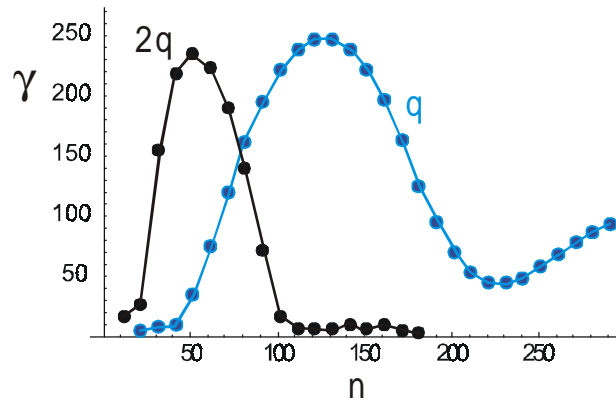


Fig. 2

Scaling of the unstable spectrum with  $q$ . Shown is the growth rate  $\gamma$  ( $10^3/s$ ) vs.  $n$  for the base case and for a case with plasma current  $I_p$  reduced by a factor of 2 (i.e.  $q$  increased by 2). The flux surface is at  $x = -0.3$  cm for this and subsequent scaling runs.

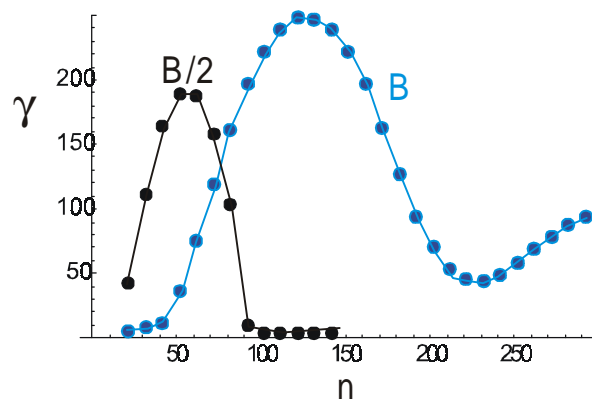


Fig. 3

Scaling of the unstable spectrum with B. Shown is the growth rate  $\gamma$  ( $10^3/s$ ) vs.  $n$  for the base case and for a case with toroidal magnetic field B reduced by a factor of 2. Here  $q$  is held constant.

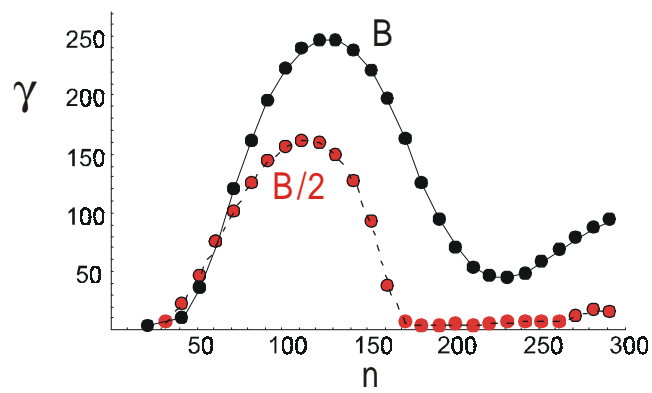


Fig. 4

Scaling of the unstable spectrum with  $B_\zeta$  at fixed  $I_p$ . Shown is the growth rate  $\gamma$  ( $10^3/s$ ) vs.  $n$  for the base case and for a case with toroidal magnetic field  $B_\zeta$  reduced by a factor of 2.

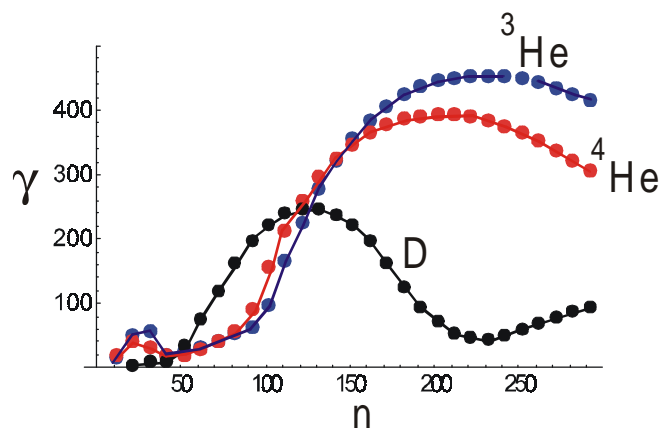


Fig. 5

Scaling of the unstable spectrum with  $Z$  and  $\mu$ . Shown is the growth rate  $\gamma$  ( $10^3/s$ ) vs.  $n$  for various ion species. The base case (D) and cases for pure  ${}^4\text{He}$  and  ${}^3\text{He}$  plasmas are shown. Here  $n_e$  is held constant.

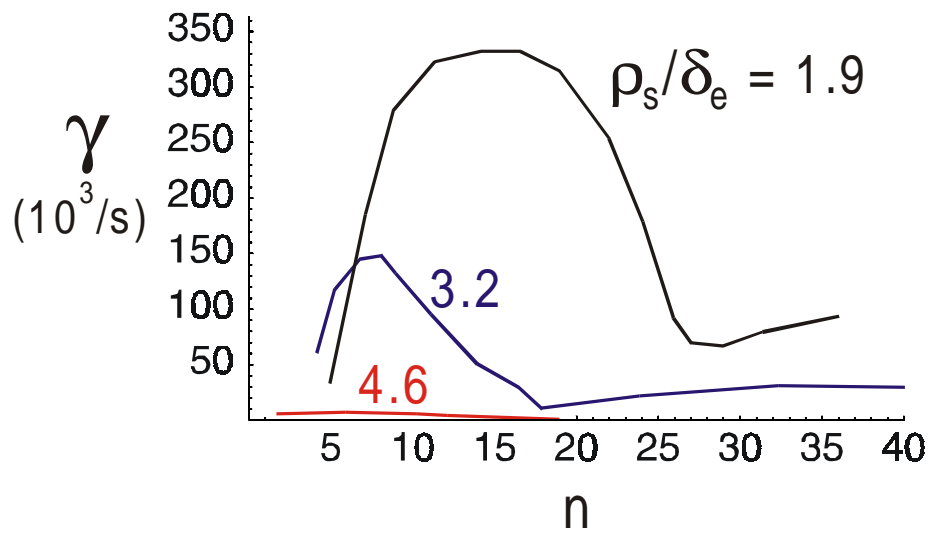


Fig. 6

Growth rate  $\gamma(10^3/s)$  vs.  $n$  for a sequence of runs with increasing pressure (edge  $\beta$ ), starting from the high-performance (high  $\beta$ , steep pedestal) parameters given in Sec. III E.



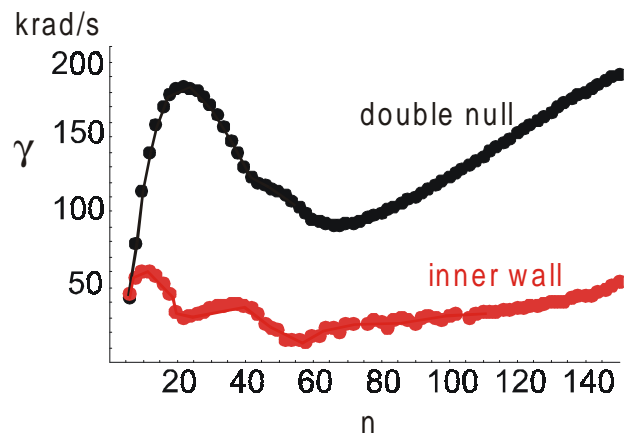


Fig. 7

Dependence of the unstable spectrum on magnetic configuration. Shown is the growth rate  $\gamma$  ( $10^3/s$ ) vs.  $n$  for the DN base case, and for an inner wall limited case on a typical flux surface ( $x = 1$  cm) in the SOL.